

Article

Cytotoxicity and Antiviral Properties of Alkaloids Isolated from *Pancreaticum maritimum*

Marco Masi ¹, Roberta Di Lecce ¹, Natacha Mérindol ², Marie-Pierre Girard ², Lionel Berthoux ³, Isabel Desgagné-Penix ^{2,4}, Viola Calabrò ⁵ and Antonio Evidente ^{1,*}

¹ Dipartimento di Scienze Chimiche, Università di Napoli Federico II, Complesso Universitario Monte Sant'Angelo, 80126 Napoli, Italy; marco.masi@unina.it (M.M.); roberta.dilecce@unina.it (R.D.L.)

² Département de Chimie, Biochimie et Physique, Université du Québec à Trois-Rivières, Trois-Rivières, QC G8Z 4M3, Canada; natacha.merindol@uqtr.ca (N.M.); marie-pierre.girard@uqtr.ca (M.-P.G.); isabel.desgagne-penix@uqtr.ca (I.D.-P.)

³ Département de Biologie Médicale, Université du Québec à Trois-Rivières, Trois-Rivières, QC G8Z 4M3, Canada; lionel.berthoux@uqtr.ca

⁴ Groupe de Recherche en Biologie Végétale, Université du Québec à Trois-Rivières, Trois-Rivières, QC G8Z 4M3, Canada

⁵ Dipartimento di Biologia, Università di Napoli Federico II, Complesso Universitario Monte Sant'Angelo, 80126 Napoli, Italy; vcalabro@unina.it

* Correspondence: evidente@unina.it

Abstract: Ten Amaryllidaceae alkaloids (AAs) were isolated for the first time from *Pancreaticum maritimum* collected in Calabria region, Italy. They belong to different subgroups of this family and were identified as lycorine, which is the main alkaloid, 9-*O*-demethyllycorine, haemanthidine, haemanthamine, 11-hydroxyvittatine, homolycorine, pancracine, obliquine, tazettine and vittatine. Haemanthidine was isolated as a scalar mixture of two 6-epimers, as already known also for other 6-hydroxycrinine alkaloids, but for the first time they were separated as 6,11-*O,O'*-di-*p*-bromobenzoyl esters. The evaluation of the cytotoxic and antiviral potentials of all isolated compounds was undertaken. Lycorine and haemanthidine showed cytotoxic activity on Hacat cells and A431 and AGS cancer cells while, pancracine exhibited selective cytotoxicity against A431 cells. We uncovered that in addition to lycorine and haemanthidine, haemanthamine and pancracine also possess antiretroviral abilities, inhibiting pseudotyped human immunodeficiency virus (HIV)–1 with EC₅₀ of 25.3 μM and 18.5 μM respectively. Strikingly, all the AAs isolated from *P. maritimum* were able to impede dengue virus (DENV) replication (EC₅₀ ranged from 0.34–73.59 μM) at low to non-cytotoxic concentrations (CC₅₀ ranged from 6.25 μM to >100 μM). Haemanthamine (EC₅₀ = 337 nM), pancracine (EC₅₀ = 357 nM) and haemanthidine (EC₅₀ = 476 nM) were the most potent anti-DENV inhibitors. Thus, this study uncovered new antiviral properties of *P. maritimum* isolated alkaloids, a significant finding that could lead to the development of new therapeutic strategies to fight viral infectious diseases.

Keywords: Amaryllidaceae; *Pancreaticum maritimum*; alkaloids; Dengue virus; human immunodeficiency virus; biological activity

Key Contribution: Ten Amaryllidaceae alkaloids belonging to different subgroups were isolated from *Pancreaticum maritimum*. For the first time the two epimers constituent the scalar mixture of haemanthidine were separated as di-*p*-bromobenzoyl esters. All the alkaloids were tested for their cytotoxic and antiviral activity and were able to impede dengue virus replication at low non-cytotoxic concentrations. Furthermore, lycorine, haemanthidine, haemanthamine, and pancracine also showed antiretroviral abilities, inhibiting pseudotyped human immunodeficiency virus (HIV).

1. Introduction

Plants belonging to the Amaryllidaceae family are distributed in Northern and Southern hemispheres, but they essentially grow in Andean South America, in the Mediterranean



Citation: Masi, M.; Di Lecce, R.; Mérindol, N.; Girard, M.-P.; Berthoux, L.; Desgagné-Penix, I.; Calabrò, V.; Evidente, A. Cytotoxicity and Antiviral Properties of Alkaloids Isolated from *Pancreaticum maritimum*. *Toxins* **2022**, *14*, 262. <https://doi.org/10.3390/toxins14040262>

Received: 14 March 2022

Accepted: 2 April 2022

Published: 7 April 2022

Publisher's Note: MDPI stays neutral with regard to jurisdictional claims in published maps and institutional affiliations.



Copyright: © 2022 by the authors. Licensee MDPI, Basel, Switzerland. This article is an open access article distributed under the terms and conditions of the Creative Commons Attribution (CC BY) license (<https://creativecommons.org/licenses/by/4.0/>).

Basin, and in South Africa [1]. They are bulbous flowering plants including approximately 1600 species classified into about 75 genera [2]. These plants were used from ancient times for their beautiful flowers and essential oils. They are widely utilized in folk medicine because of the diverse and powerful therapeutic activities exhibited by their extracts and decoctions [3,4]. Many of these biological activities are due to their content in alkaloids that are present mostly in the plant bulbs [4–6].

The Amaryllidaceae alkaloids (AAs) are grouped in 12 ring types [7,8]. The extensive use of AAs producing plants in folk medicine and their varied carbon skeleton prompted a deep investigation into their potential as phytochemical-based drug discovery [9]. Hundreds of AAs with different carbon skeletons and functionalities have been isolated [1,5,6,8–10]. Among them, many have shown promising anticancer activity [11], as lycorine- and its related isocarbostryl narciclasine [12–18], crinine- [19–21], pretazettine- [22], and montanine- [23] type alkaloids. Many AAs also possess anti-acetylcholinesterase potential such as sanguinine isolated from *Crinum giganteum* [24] or galanthamine currently used as a cholinesterase inhibitor drug to treat Alzheimer's disease [25]. Other AAs possess anti-parasitic [26], anti-larvicidal and anti-insecticidal [27,28] properties. Some AAs display broad antiviral activity, i.e., lycorine, haemanthamine and 11-hydroxyvittatine inhibit the replication of influenza virus H5N1 [29], haemanthamine, lycorine and homolycorine were also shown to display antiretroviral activities [30], while lycorine and derivatives are potent inhibitors of flaviviruses and coronaviruses. Recently, we also showed that cherylline was a potent anti-flaviviral compound [31]. To date, there are no antiviral drugs approved to treat flaviviral infections such as dengue fever caused by the Dengue virus (DENV) that affects 400 million people each year. Moreover, despite a highly efficacious combined antiretroviral therapy, there are still no curative agents for the 37.87 million people living with HIV-1 that must take their medication all their life to prevent viral replication. Thus, the characterization of AAs antiviral activities is at the front line for new drug discovery.

Recent studies emphasized the importance of investigating either uncharacterized species or known species but collected in different regions of the world to grasp Amaryllidaceae's diverse potential as a source of AAs.

Studies on the alkaloids produced by *Pancreatum maritimum* started in 1954 with the investigation performed by du Merac (1954) [32]. Subsequently, investigations allowed to isolate alkaloids belonging to the subgroups lycorine-, lycorenine-, montanine-tazettine- galanthamine- haemanthidine- and crinine-, isocarbostryl as narciclasine- and pancratistatin-type [33]. In particular, 40 alkaloids were isolated from bulbs and leaves extracts of *P. maritimum* collected in Turkey, Egypt, Italy (Apulia region) and Bulgaria, showing purgative, acaricidal, insecticidal, and antifungal activities [34]. Among them, (-)-3b,11a-dihydroxy-1,2-dehydrocrinane and (-)-8-hydroxy-9-methoxycrinine trisphaeridine, pancratimines A, B and C, and norismine, were isolated [35]. In other studies, ungeremine and zefbetaine were isolated [36], as well as narciclasine-4-O- β -D-glucopyranoside [37]. Ungeremine exhibited significant bactericidal activity against the Gram-negative *Flavobacterium columnare* causing channel catfish (*Ictalurus punctatus*) columnaris disease [38]. Furthermore, ungeremine was bioformulated in chitosan tripolyphosphate which was particularly active against *Penicillium roqueforti*, a fungus responsible for bakery products deterioration [39,40].

Considering that organic plant extracts show a high level of variability in their composition depending on several factors (e.g., geographical origin, inter- and intra-specific genetic variability, plant phenologic stage), and the need for new therapeutics to treat human diseases, a new investigation of the alkaloid content of *P. maritimum* collected for the first time in Calabria region, Italy, was carried out (Figure 1).

This study reports the identification of ten alkaloids isolated from the acid bulb extract of *P. maritimum* and for the first time describes the separation of the two 6-epimers of haemanthidine as *p*-bromobenzoyl derivatives, which also allowed us to assign their relative and absolute configuration. The results of their cytotoxic and antiviral properties were also described.

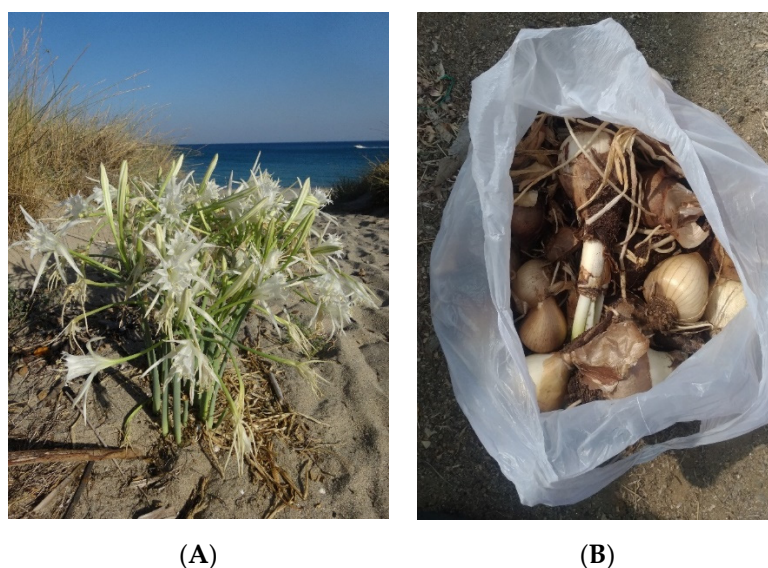


Figure 1. Flowers (A) and bulbs (B) of *Pancratium maritimum*.

2. Results and Discussion

Dried and minced *P. maritimum* bulbs were acid extracted and the aqueous phase was re-extracted with EtOAc following alkalization, as detailed in Experimental section. Evaporation of the solvent left an oily residue which was crystallized and yielded an abundant amount of lycorine (**1**, Figure 2), the main isolated metabolite. The mother liquors resulting from lycorine crystallization were evaporated under reduced pressure, yielding a residue which was purified using a combination of column and TLC chromatography on silica gel, allowing us to isolate ten already known AAs identified as tazettine, homolycorine, obliquine, vittatine, haemanthamine, haemanthidine, 9-*O*-demethylhomolycorine, 11-hydroxyvittatine and pancracine (**2–10**, Figure 2), thus belonging to lycorine- (**1**), pretazettine- (**2**), homolycorine- (**3**, **4** and **8**), crinine- (**5–7** and **9**) and pancracine- (**10**) types.

These alkaloids were identified comparing their physical (specific optical rotation) and spectroscopic (^1H and ^{13}C NMR and ESI MS) properties with those already reported in the literature: for **1** by Lamoral-Theys et al. (2009) [13] isolated from *Stenbergia lutea*, for **2** with those reported by Antoun et al. (1993) [41] and Boit and Döpke (1960) [42] when isolated from *Hymenocallis expansa* and *Hippeastrum aulicum*, respectively. Alkaloids **3** and **4** were identified by comparing our experimental results with those reported by Fales et al. (1956) [43], Furosawa et al. (1976) [44] and Baxendale and Lei (2005) [45] when isolated from *Narcissus tazetta* and *Cyrtanthus obliquus*. Alkaloids **5** and **6** were identified comparing our data with those reported by Frahm et al. (1985) [46], Bastida et al. (1995) [47], Pabuçcuoglu et al. (1989) [48] and Ghosal et al. (1985) [49] when isolated from *Crinum asiaticum*, *Narcissus cantabricus* and *Stenbergia sicula*, respectively. Likewise, alkaloids **7** and **8** were identified by comparing their data with those described by Ma et al. (1986) [50], Antoun et al. (1993) [41], Forgo and Hoffmann (2005) [51], Bastida et al. (1987) [52] and Evidente et al. (1994) [53] when isolated from *Hymenocallis expansa*, *Narcissus tazetta* L. var *chinensis* roem, *Leucojum vernum* and *Narcissus confusus*, respectively. Finally, alkaloids **9** and **10** were identified by comparison with those reported by Evidente (1986) [54] and Ali et al. (1984) [55] when isolated from *Hippeastrum vittatum* and *Stenbergia lutea*, respectively. Interestingly, among all the alkaloids isolated in this study, obliquine (**4**) and pancracine (**10**) were isolated for the first time from *P. maritimum*.

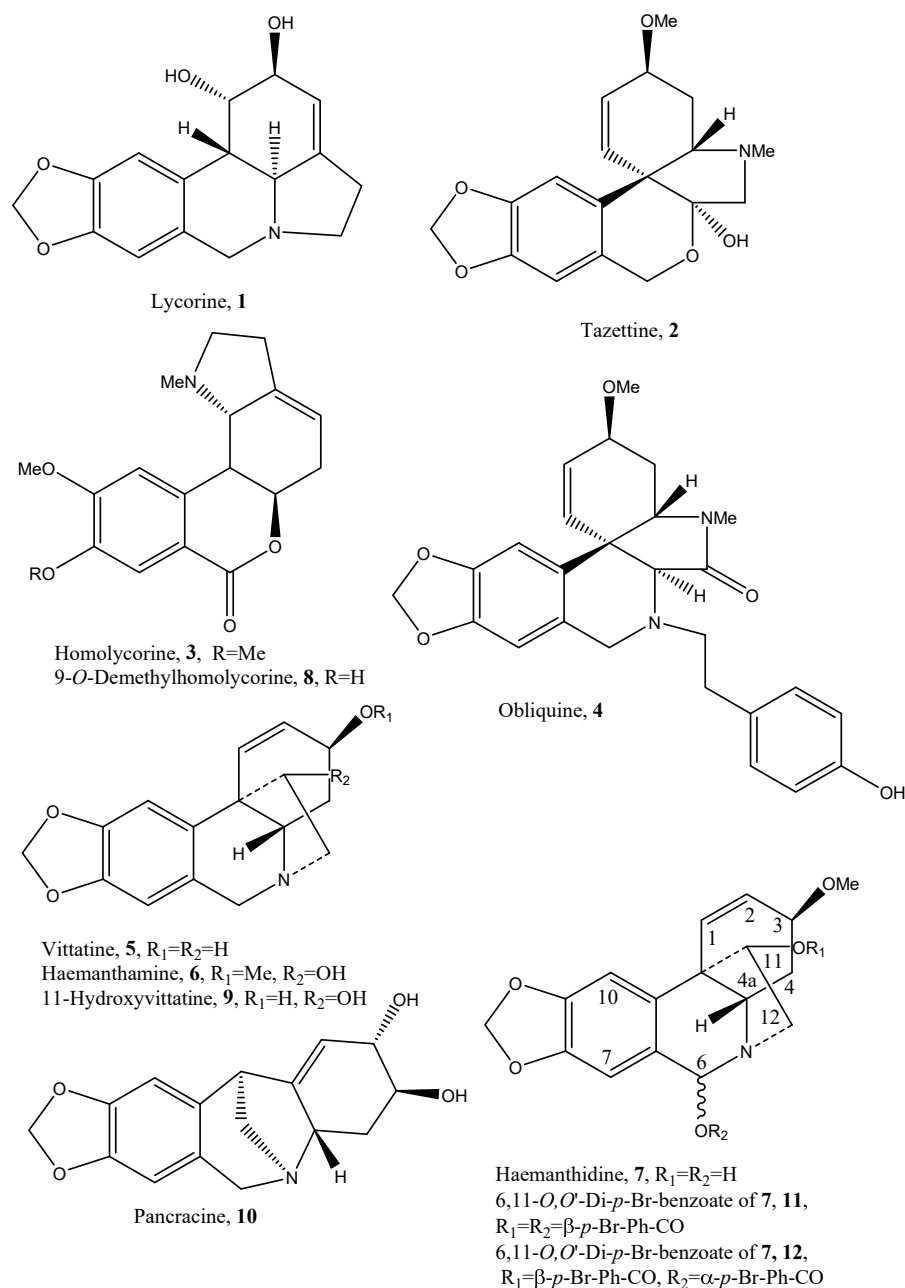


Figure 2. Structures of lycorine, tazettine, homolycorine, obliquine, vittatine, haemanthamine, haemanthidine, 9-O-demethylhomolycorine, 11-hydroxyvittatine, pancracine (1–10) isolated from *P. maritimum* and that of the two diastereomeric *p*-bromobenzoyl esters of 7 (11 and 12).

As previously reported, haemanthidine (7) was isolated as two 6-epimers [56] in a scalar ratio. The equilibrium between the two epimers was also reported for 6-hydroxycrinamine, but not for closely related crinine-type alkaloids such as 6 α -hydroxycrinine and 6 α -hydroxybuphonisine. The equilibrium between the two epimers could be explained through their interconversion in solution via the corresponding aminoaldehyde [57]. The ratio of the two epimers in solution, evidenced by ¹H NMR spectroscopy, is affected from the variable temperature at which the spectrum is recorded. Haemanthidine (7) epimeric ratio was of 2:1, whereas King et al. (1965) [57] observed a 1:1 ratio. Any attempt to separate the two 6-epimers and to determine their absolute configuration failed. In addition, their esters were not separable upon converting the mixture of 6-epimers in the corresponding 6,11-O,O'-diacetyl derivatives. Instead, when converted by reaction with *p*-bromobenzoyl

chloride in the usual conditions, haemanthidine yielded two corresponding epimeric esters (**11** and **12**, Figure 2) which were easily separated by TLC chromatography and characterized by physic properties (specific optical rotation), ^1H NMR and ESI MS spectroscopy. The comparison of the two ^1H NMR spectra (Table 1) of **11** and **12** with that of **7** showed as substantial difference the presence of the signal pattern of a *p*-disubstituted phenyl residue, appearing as two couples of doublets ($J = 8.2$ and $J = 8.6$ Hz) at δ 7.93 and 7.60 ($2',6'$ and $3',5'$) and 7.77 and 7.58 ($2'',6''$ and $3'',5''$) for **11**, and ($J = 8.4$ and $J = 8.7$ Hz) at δ 8.00 and 7.62 ($2',6'$ and $3',5'$), and 7.77 and 7.59 ($2'',6''$ and $3'',5''$) for **12**.

Table 1. ^1H NMR Data of the two 6,11-*O,O'*-Di-*p*-Bromobenzoyl Esters (**11** and **12**) ^{a,b} of haemanthidine (**7**).

	11	12
No.	δ_{H} (J in Hz)	δ_{H} (J in Hz)
1	6.40 d (10.4)	6.39 d (10.1)
2	6.15 dd (10.4; 4.8)	6.13 dd (10.1, 5.0)
3	3.84 m	3.84 m
4	2.05 m (2H)	2.18 m (2H)
4a	3.80 dd (13.0, 5.1)	3.75 dd (12.7, 5.0)
6	6.38 s	6.93 s
7	6.99 s	6.97 s
10	6.71 s	6.66 s
11	5.18 dd (7.0, 3.6)	5.20 dd (6.9, 2.7)
12	3.70 dd (14.9, 7.0)	4.12 dd (14.8, 6.9)
	3.53 dd (14.9, 3.6)	3.21 dd (14.8, 2.7)
OCH ₂ O	5.96 s	5.96 s
	5.95 s	5.95 s
OMe	3.34 s (3H)	3.33 s (3H)
2',6'	7.93 d (8.2) (2H)	8.00 d (8.4) (2H)
3',5'	7.60 d (8.2) (2H)	7.62 d (8.4) (2H)
2'',6''	7.77 d (8.6) (2H)	7.77 d (8.7) (2H)
3'',5''	7.58 d (8.6) (2H)	7.59 d (8.7) (2H)

^a The chemical shifts are in δ values (ppm) from TMS. ^b 2D ^1H , ^1H (COSY) NMR experiment confirmed the coupling of all the protons.

Furthermore, the expected significant downfield shifts H-6 and H-11 were observed. In particular, in the spectrum of **11**, H-6 and H-11 appeared as a singlet and a double doublets ($J = 7.6$ and 3.6 Hz) downfield shifted ($\Delta\delta$ 1.27 and 1.23) with respect to **7** at δ 6.38 and 5.18, similarly in **12**, the same signal appeared as a singlet (H-6) and a double doublet ($J = 6.9$ and 2.7 Hz) (H-11) downfield shifted ($\Delta\delta$ 1.18 and 1.25) with respect to **7** at δ 6.93 and 5.20, respectively.

Furthermore, **11** and **12**, as expected showed the same typical ESI MS spectrum exhibiting the three peaks due the presence of the two isotopes of the two bromine at m/z 696 $[\text{M} + \text{H}]^+$, 698 $[\text{M} + 2 + \text{H}]^+$, 700 $[\text{M} + 4 + \text{H}]^+$.

The NOESY spectra (Table 2) of **11** and **12** showed both the expected correlations of H-1 with H-10 and H-2, H-2 with H-3, the latter with H₂-4 and MeO, H-11 with H-12A and the latter with H-12B. There was a significant difference with regards to the correlation observed in **12** between H-6 and H-4a, which was absent in **11**. This last result allowed us to assign the same β -orientation of H-6 as H-4a in **12**, while in **11** H-6 resulted to be α -located. Thus, knowing the absolute configuration of other chiral centers of haemanthidine [58], H-6 has a *S*-configuration in **12** and an *R*-configuration in **11**. All the attempts to recover the *p*-bromobenzoyl esters in the free base **7** by hydrolysis carried out in different conditions failed.

Table 2. ¹H NOESY NMR Data for the two 6,11-*O,O'*-Di-*p*-Bromobenzoyl Esters of Haemanthidine (**11** and **12**)^a.

11		12	
Irradiated	Observed	Irradiated	Observed
H-1	H-10, H-2	H-1	H-10, H-2
H-2	H-3	H-2	H-3
H-6	H-12A	H-6	H-4a, H-12A
H-3	H ₂ -4, MeO	H-3	H ₂ -4, MeO
H-11	H-12A	H-11	H-12A
H-12A	H-12B	H-12A	H-12B

^a The chemical shifts are in δ values (ppm) from TMS.

Previous literature reported that several AAs, including haemanthidine as a 6-epimer mixture displayed cytotoxic potential against several types of cancer cell lines [59] and the growth inhibitory effect on both parental and multidrug resistant L5178 mouse lymphoma cell lines [60]. Thus, the cytotoxic activity was assessed for all the isolated alkaloids (**1–6** and **8–10**), the scalar 6-epimer mixture of **7** and their two ester **11** and **12**.

The potential cytotoxic activity of *P. maritimum* alkaloids was evaluated on Hacat, A431 and AGS cells treated with concentrations ranging from 0.5 to 10 μ M for 24 and 48 h by measuring the reduction of 3-(4,5-dimethylthiazol-2) 2,5- diphenyltetrazolium bromide (MTT) to formazan by the mitochondrial enzyme succinate dehydrogenase. We selected Hacat cells because they are spontaneously immortalized human keratinocytes and they have been used in several studies as a paradigm for non-transformed epidermal cells. A431 and AGS cells were chosen as transformed epithelial cells derived from skin epidermoid tumor and gastric carcinoma, respectively. Interestingly, as shown in Figures 3 and 4, in addition to lycorine ($IC_{50} < 0.5 \mu$ M), AGS cells were sensitive to haemanthamine (**6**) ($IC_{50} = 7.5 \mu$ M at 24 and 48 h) and haemanthidine (**7**) ($IC_{50} = 5.0 \mu$ M at 24 h), albeit at much higher concentrations (Table 3).

We further evaluated the cytotoxic activity of the two *p*-bromobenzoyl derivatives (**11**, **12**) of haemanthidine with concentrations ranging from 0.5 to 50 μ M for 24 and 48 h. As shown in Figure 4, both epimers were able to reduce AGS cell viability.

The only alkaloid with cytotoxic activity on Hacat and A431 cells was lycorine ($IC_{50} = 0.5 \mu$ M at 48 h for both cell lines). Indeed, we only observed a slight to moderate reduction of Hacat and A431 cell viability (between 15–30%) with 10 μ M haemanthidine, -*O*-demethylhomolycorine, haemanthamine and tazettine at 24 h of treatment. At 48 h, cell growth was almost completely rescued suggesting that cells underwent a reversible cell cycle arrest. This suggest that haemanthidine and haemanthamine could display a selective toxicity towards cancer cells.

Among the alkaloids isolated from *P. maritimum* in this study, several have been associated with antiviral functions, while others have not been tested. Lycorine, haemanthamine and 11-hydroxyvittatine were reported to inhibit the replication of influenza virus H5N1 [29]. Haemanthamine, lycorine and homolycorine were also shown to display antiretroviral activities [30], while lycorine and derivatives are potent inhibitors of flaviviruses and coronaviruses. In this study, we assessed the antiviral activity of all the isolated alkaloids (**1–6** and **8–10**) and the scalar 6-epimer mixture of **7**. We focused on the antiretroviral and anti-flaviviral activities, as we and others have previously shown that several AAs efficiently target HIV-1 and DENV replication (Figure 5).

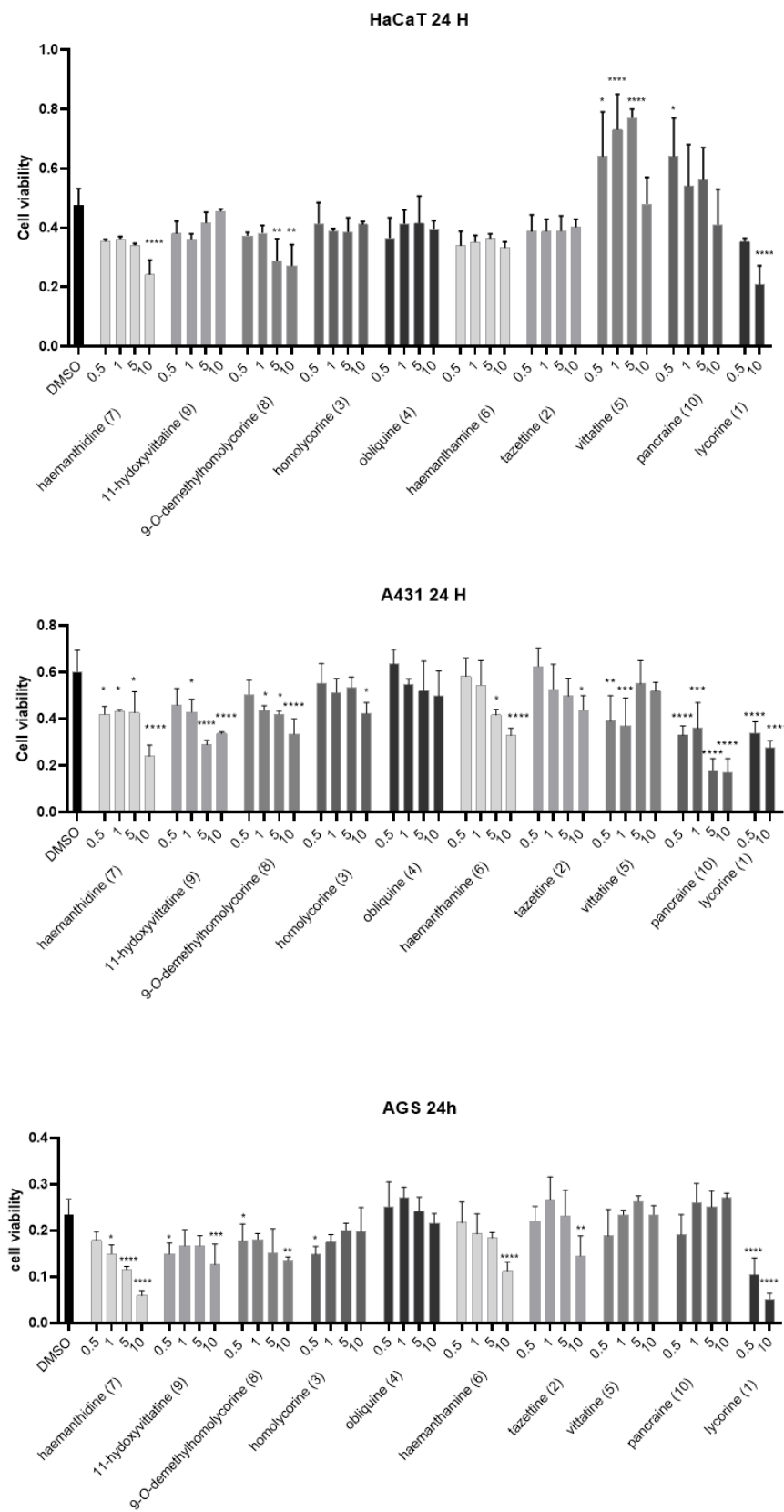


Figure 3. MTT viability test. HacaT, A431 and AGS cells were incubated with the indicated amounts of alkaloids in DMSO, for 24 h. The values were the mean's six values for each experimental point of biological replicates. Each mean was compared using a Dunnett's multiple comparisons test of ANOVA one-way (p -value $*$ < 0.01, $**$ < 0.05, $***$ p < 0.001; $****$ p < 0.0001). DMSO control.

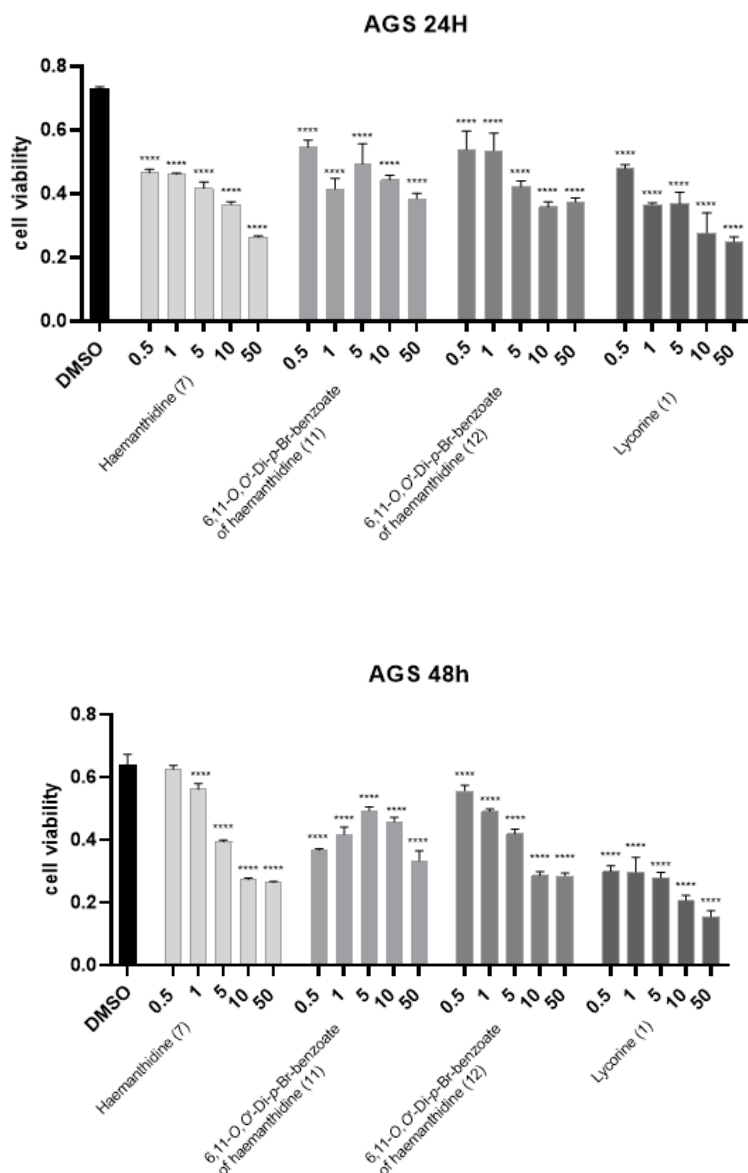


Figure 4. MTT viability test of *P. maritimum* alkaloid. AGS cells were incubated with the indicated amount of haemantidine (7), β-epimer (11), α-epimer (12), and lycorine (1) in DMSO, for 24 h (upper panel) or 48 h (lower panel). The values were the mean’s six values for each experimental point of biological replicates. Each mean was compared using a Dunnett’s multiple comparisons test of ANOVA one-way (*p*-value **** *p* < 0.0001). DMSO control.

Table 3. IC₅₀ values of tested compounds.

IC ₅₀	Hacat	A431	AGS
Lycorine	0.5 µM	0.5 µM	<0.5 µM
Haemanthamine	-	-	IC ₅₀ = 7.5 µM
Haemantidine	-	-	IC ₅₀ = 5.0 µM

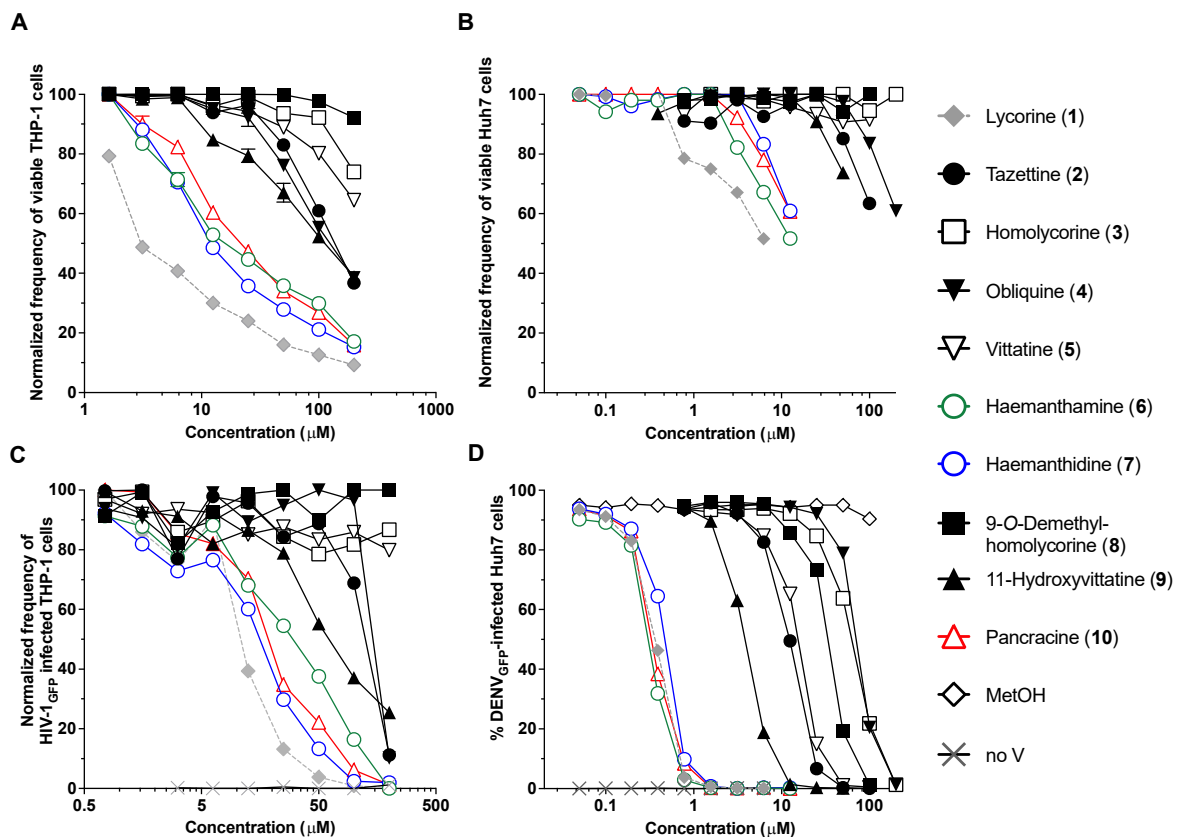


Figure 5. Antiviral assays. (A) Cytotoxicity of *P. maritimum*'s isolated compounds measured in THP-1 cells. (B) Cytotoxicity in Huh7 cells. Cell viability was assessed by measuring ATP levels. The frequency of viable cells is expressed as a percentage of ATP levels in cells treated with alkaloids normalized to cells treated with matched concentrations of vehicle methanol. Wells without cells were used as negative controls. (C) Anti-retroviral potential of isolated compounds. Alkaloid-treated THP-1 cells were infected with HIV-1_{GFP} at an MOI = 0.1. Infection levels were measured 72 h later and normalized using methanol treated cells. Raltegravir (10 μM) used as a positive control completely impeded HIV-1 infection. (D) Anti-flaviviral potential of isolated compounds. DENV_{GFP} (MOI = 0.02) was used to infect Huh7 cells treated with alkaloids. Infection levels were measured 72 h later. Shown are representative results of three independent experiments.

To account for non-specific antiviral activity caused by enhanced cell death, the cytotoxicity of *P. maritimum* isolated AAs was first determined in THP-1 and Huh7 virus-targeted cell lines exposed to concentrations ranging from 0.05 to 200 μM for 72 h. Cell viability was measured using ATP levels as a marker. The most cytotoxic compounds were lycorine, haemanthamine, pancracine, haemanthidine, followed by 11-hydroxyvittatine, tazettine and obliquine in both THP-1 and Huh7 cells (Figure 5A,B). In THP-1 cells used for HIV-1 infection, lycorine (CC_{50} = 4.6 μM) impacted cell viability at all concentrations whereas haemanthidine (CC_{50} = 16.8 μM), haemanthamine (CC_{50} = 22.2 μM) and pancracine (CC_{50} = 25.93 μM), decreased cell viability beginning at 3.125 μM with 71%, 71% and 82% of live cells at 6.25 μM , respectively. A concentration of 100 μM of obliquine, tazettine and 11-hydroxyvittatine reduced viable THP-1 cells to 55.3%, 60.9% and 52.3%, respectively (Figure 5A and Table 3). In the Huh7 cells used for DENV infection, 0.78 μM of lycorine reduced viability by 21%, while haemanthamine was cytotoxic at concentrations above 3.125 μM (82.2% live cells), and pancracine and haemanthidine decreased viability beginning at 6.25 μM (78.1% and 83.3% of live cells, respectively). 11-hydroxyvittatine and tazettine reduced viability at concentrations higher than 50 μM (73.8% and 85.2% viable cells, respectively) and obliquine was toxic from 100 μM (82.6%) (Figure 5B). The AAs CC_{50} were not reached at the concentrations used in our assays.

Next, pseudotyped HIV-1_{GFP} vectors were used to assess the antiretroviral potential of alkaloids. These vectors enter THP-1 cells, reverse transcribe their viral RNA, integrate viral DNA into the host genome, produce viral proteins and GFP, but do not lead to the production of infectious viral particles. We treated THP-1 cells with each AA and infected them at an MOI = 0.1 (Figure 5C). The percentage of infected GFP⁺ THP-1 cells was measured 72 h post-infection using a flow cytometer. Lycorine, haemanthamine, pancracine, haemanthidine, 11-hydroxyvittatine, tazettine and obliquine displayed a dose-dependent inhibition of HIV-1. Complete viral inhibition was observed for haemanthidine, lycorine, haemanthamine, and pancracine at 100 μ M (Figure 5C) with EC₅₀ of 12.7 μ M, 10.9 μ M, 25.3 μ M, 18.5 μ M, respectively (Figure 5C and Table 4). Whereas haemanthamine and lycorine have been previously reported to display antiretroviral activities [30], our results suggest that haemanthidine and pancracine also share this function. However, and for all four alkaloids, only 40–50% of cells remain viable at the EC₅₀. Thus, although these alkaloids display interesting antiretroviral effects as previously reported, the effective concentrations to block infection are considerably cytotoxic.

Table 4. *P. maritimum* alkaloids antiviral activity. EC₅₀ and CC₅₀ were calculated with QuestGraph IC₅₀ Calculator, with concentrations ranging from 0.5 to 200 μ M for HIV-1_{GFP} and from 0.05 to 200 μ M for DENV_{GFP}.

Alkaloids	EC ₅₀ (μ M)		CC ₅₀ (μ M)
	DENV _{GFP}	HIV _{GFP}	THP-1
Lycorine	0.39	10.90	4.61
9-O-Demethylhomolycorine	34.49	nd	nd
Homolycorine	65.03	nd	nd
Tazettine	12.50	120.30 *	136.90
Vittatine	15.53	nd	nd
11-Hydroxyvittatine	3.92	65.10 *	113.06
Haemanthamine	0.34	25.27	22.19
Haemanthidine	0.48	12.74	16.80
Pancracine	0.36	18.51	25.93
Obliquine	73.59	152.86 *	127.04

CC = cytotoxic concentration, EC = Effective concentration, * Incomplete inhibition; nd: not detected.

Lycorine is recognized for its anti-flaviviral properties. We assessed AAs' anti-flavivirus properties using the DENV_{GFP} dengue vector, which is propagation-competent. Upon infection, this vector leads to the production of GFP concomitantly with the translation of viral genomic RNA. Infection was measured by assessing the % of GFP⁺ cells 72 h post-infection on a flow cytometer (Figure 5D). Obliquine (4) (EC₅₀ = 73.6 μ M), homolycorine (3) (EC₅₀ = 65.0 μ M), 9-O-demethylhomolycorine (8) (EC₅₀ = 34.49 μ M), vittatine (5) (EC₅₀ = 15.53 μ M), tazettine (2) (EC₅₀ = 12.5 μ M), 11-hydroxyvittatine (9) (EC₅₀ = 3.92 μ M), haemanthidine (7) (EC₅₀ = 0.476 μ M), lycorine (1) (EC₅₀ = 0.386 μ M), pancracine (10) (EC₅₀ = 0.358 μ M), and haemanthamine (6) (EC₅₀ = 0.337 μ M) all impeded DENV_{GFP} replication. Complete inhibition was obtained at 1.56 μ M for lycorine, haemanthamine, pancracine and haemanthidine. At this concentration, only lycorine was cytotoxic at detectable levels, reducing cell viability by 25% (Figure 5B,D). To our knowledge, this is the first report on these AAs inhibiting flavivirus at levels comparable to lycorine and less cytotoxicity. Thus, we have uncovered that *Pancreatium maritimum*'s extracted haemanthamine, haemanthidine and pancracine are potent antflaviviral compounds that should be further explored.

3. Conclusions

This manuscript reports an in-depth investigation of *P. maritimum* isolated from the first time in South Italy Coast. Ten already known Amaryllidaceae alkaloids belonging to different subgroups were identified as lycorine, the main alkaloid, 9-O-demethyllycorine, haemanthidine, haemanthamine, 11-hydroxyvittatine, homolycorine, pancracine, obliquine, tazettine and vittatine, with obliquine and pancracine isolated for the first time from this

Amaryllidaceae. Lycorine and haemanthidine showed cytotoxic activity on Hacat cells and A431 and AGS cancer cells while, pancracine exhibited selective cytotoxicity against A431 cells. Finally, we uncovered that *P. maritimum*'s isolated haemanthamine, haemanthidine and pancracine display promising antiviral activity.

4. Materials and Methods

4.1. General Experimental Procedures

Optical rotations were measured in a MeOH solution on a Jasco P-1010 digital polarimeter (Jasco, Tokyo, Japan). ^1H and ^{13}C NMR spectra were recorded at 400 and 100 MHz, respectively, in CD_3OD or otherwise noted on a Bruker spectrometer (Bruker, Karlsruhe, Germany). The same solvent was used as an internal standard. and Nuclear Overhauser Effect Spectroscopy (NOESY) experiments [61] were performed using Bruker microprograms; ESI mass spectra and liquid chromatography (LC)/MS analyses were performed using the LC/MS TOF system Agilent 6230B, HPLC 1260 Infinity (Agilent, Milan, Italy). The HPLC separations were performed with a Phenomenex LUNA (C18 (2) $5\ \mu\text{m}$ $150 \times 4.6\ \text{mm}$). Analytical and preparative Thin-Layer Chromatography (TLC) was performed on silica gel plates (Merck, Darmstadt, Germany, Kieselgel 60, F254, 0.25 and 0.5 mm, respectively) or on reverse phase (Whatman, Maidstone, UK, KC18 F254, 0.20 mm) plates and the compounds were visualized by exposure to UV light and/or iodine vapors CC: silica gel (Merck, Darmstadt, Germany, Kieselgel 60, 0.063–0.200 mm).

4.2. Plant Material

Bulbs of *Pancreatum maritimum* were collected in Squillace, Italy ($38^\circ 47' 20.6''\ \text{N}$ and $16^\circ 35' 10.8''\ \text{W}$), in August 2020 (Figure 1). The plant specimen is deposited in the collection of the same Department of Biology, University of Naples Federico II.

4.3. Extraction and Purification of Alkaloids

Fresh bulbs of *P. maritimum* (6 kg) were dried at room temperature and then finely powdered. The resulting powder (736.2 g) was extracted with 1% H_2SO_4 , ($2 \times 1\ \text{L}$) overnight at room temperature. The suspension was filtered through cloth and successively centrifuged at $10\ ^\circ\text{C}$ at 7000 rpm for 30 min. The acid extract was alkalized to pH 9–10 with 12 N NaOH. The aqueous solution was extracted with EtOAc ($3 \times 1\ \text{L}$), and the organic extracts were combined, dried (Na_2SO_4) and evaporated under reduced pressure to give a brown oil residue (3.9 g). This latter was crystallized by EtOH obtaining lycorine (**1**, 900 mg) as white crystals. The mother liquors of crystallization were dried, and the residue (3.0 g) was fractionated by column chromatography eluted with CHCl_3 -EtOAc-MeOH (2:2:1), affording eight groups of homogeneous fractions (F1–F8). The residue (182.5 mg) of fraction F3 was purified on silica gel column chromatography (CC) eluted with CHCl_3 -*i*-PrOH (9:1), yielding five fractions (F3.1–F3.5). The residue (50.5 mg) of fraction 2 resulted to be an amorphous solid identified as tazettine (**9**). The residue (336.5 mg) of fraction F4 was purified on CC eluted with EtOAc-MeOH- H_2O (7:2:1) yielding seven homogeneous fractions (F4.1–F4.7). The residue (48.9 mg) of F4.1 was further purified by preparative TLC eluted with CHCl_3 -EtOAc-MeOH (2:2:1) obtaining an amorphous solid identified as homolycorine (**6**, 8.4 mg). The residue (15.6 mg) of F4.3 was purified by TLC eluted with CHCl_3 -EtOAc-MeOH (2:2:1) yielding obliquine (**8**, 4.6 mg) as an amorphous solid. The residue (546.6 mg) of F5 was purified by CC eluted with EtOAc-MeOH- H_2O (7:2:1) yielding six homogeneous fractions (F5.1–F5.6). The residue (67.5 mg) of fraction F5.2 was purified on preparative TLC with CH_2Cl_2 -MeOH (8:2) yielding vittatine (**4**, 8.6 mg) and haemanthamine (**3**, 2.2 mg) as amorphous solids. The residue (97.5 mg) of fraction F5.3 was purified on preparative TLC with CHCl_3 -EtOAc-MeOH (6:2:2) yielding haemanthidine (**2**, 30.6 mg) as an amorphous solid. The residue (12.9 mg) of fraction F5.5 was purified on preparative TLC with CHCl_3 -*i*-PrOH (7:3) yielding an amorphous solid identified as 9-*O*-demethylhomolycorine (**7**, 3.3 mg). The residue (333.5 mg) of F6 was purified by CC eluted EtOAc-MeOH- H_2O (7:2:1), yielding five groups of homogeneous fractions (F6.1–F6.5). The residue (62.6 mg)

of fraction F6.3 was purified by preparative TLC eluted twice with CHCl_3 -EtOAc-MeOH (2:2:1) obtaining an amorphous solid identified as 11-hydroxyvittatine (**5**, 13.4 mg). The residue (31.2 mg) of fraction F6.4 was purified by TLC eluted with EtOAc-MeOH- H_2O (7:2:1) obtaining an amorphous solid identified as pancracine (**10**, 9.4 mg).

Lycorine (**1**). $[\alpha]_{\text{D}}^{25} -72.5$ (c 0.1, CH_3OH) [lit. [62]: $[\alpha]_{\text{D}}^{25} -71.2$ (c 0.1, CH_3OH)]; ^1H and ^{13}C NMR data are in agreement to those previously reported [13]. ESIMS (+) m/z : 288 $[\text{M} + \text{H}]^+$.

Tazettine (**2**). $[\alpha]_{\text{D}}^{25} +143.1$ (c 1.2, CHCl_3) [lit. [41]: $[\alpha]_{\text{D}}^{25} +138$ (c 0.23, CHCl_3)]; ^1H NMR (CD_3OD) data are in agreement to those previously reported [42]. ESIMS (+) m/z : 332 $[\text{M} + \text{H}]^+$.

Homolycorine (**3**). $[\alpha]_{\text{D}}^{25} +95.3$ (c 1.2, CHCl_3) [lit. [43]: $[\alpha]_{\text{D}}^{26} +93.5$ (c 1.2, CHCl_3)]; ^1H NMR (CD_3OD) data are in agreement to those previously reported [44]. ESIMS (+) m/z : 316 $[\text{M} + \text{H}]^+$.

Obliquine (**4**). $[\alpha]_{\text{D}}^{25} -135.6$ (c 0.1, CH_3OH) [lit. [45]: $[\alpha]_{\text{D}}^{25} -137.8$ (c 0.3, CH_3OH)]; ^1H and ^{13}C NMR (CDCl_3) data are in agreement to those previously reported [45]. ESIMS (+) m/z : 449 $[\text{M} + \text{H}]^+$.

Vittatine (**5**). $[\alpha]_{\text{D}}^{25} +28.0$ (c 1.2, CHCl_3) [lit. [47]: $[\alpha]_{\text{D}}^{20} +26$ (c 0.25, CH_3OH)]; ^1H NMR (CD_3OD) data are in agreement to those previously reported [46,48]. ESIMS (+) m/z : 272 $[\text{M} + \text{H}]^+$.

Haemanthamine (**6**). $[\alpha]_{\text{D}}^{25} +41.0$ (c 1.2, CHCl_3) [lit. [49]: $[\alpha]_{\text{D}}^{22} +38.3$ (c 0.45, CHCl_3)]; ^1H NMR (CD_3OD) data are in agreement to those previously reported [46,48]. ESIMS (+) m/z : 302 $[\text{M} + \text{H}]^+$.

Haemanthidine (**7**). $[\alpha]_{\text{D}}^{25} -12.2$ (c 1.2, CHCl_3) [lit. [41]: $[\alpha]_{\text{D}}^{25} -14$ (c 0.28, CHCl_3)]; ^1H and ^{13}C NMR (CDCl_3) data are in agreement to those previously reported [50]. ESIMS (+) m/z : 318 $[\text{M} + \text{H}]^+$.

9-O-Demethylhomolycorine (**8**). $[\alpha]_{\text{D}}^{25} +56.1$ (c 0.1, CHCl_3) [lit. [51]: $[\alpha]_{\text{D}}^{25} +57$ (c 0.2, CHCl_3)]; ^1H NMR (CD_3OD) data are in agreement to those previously reported [52,53]. ESIMS (+) m/z : 302 $[\text{M} + \text{H}]^+$.

11-Hydroxyvittatine (**9**). $[\alpha]_{\text{D}}^{25} +12.1$ (c 0.1, CH_3OH) [lit. [54]: $[\alpha]_{\text{D}}^{25} +11.3$ (c 0.88, CH_3OH)]; ^1H NMR (CD_3OD) data are in agreement to those previously reported [54]. ESIMS (+) m/z : 288 $[\text{M} + \text{H}]^+$.

Pancracine (**10**). $[\alpha]_{\text{D}}^{25} +72.9$ (c 0.1, CH_3OH) [lit. [55]: $[\alpha]_{\text{D}}^{25} +74$ (c 0.6, CH_3OH)]; ^1H and ^{13}C NMR (CD_3OD) data are in agreement to those previously reported [55]; ESIMS (+) m/z : 288 $[\text{M} + \text{H}]^+$.

4.4. Conversion of Haemanthidine in the Corresponding 6,11-O,O'-di-p-Bromobenzoyl Esters (**11** and **12**)

Hemanthidine, (**7**) (2.0 mg), was dissolved in CH_3CN (600 μL), and 4-dimethylaminopyridine (DMAP) (4.3 mg) and p-bromobenzoyl chloride (4.1 mg) were added. The reaction mixture was stirred at room temperature for 24 h and then evaporated under reduced pressure. The residue (10.2 mg) was purified by TLC on silica gel, eluent n-hexane-EtOAc (6:4) giving Derivatives **11** (2.3 mg), and **12** (3.8 mg), as colorless oils. **11** had: ^1H NMR, See Table 1; ESI-MS (+) m/z 696 $[\text{M} + \text{H}]^+$, 698 $[\text{M} + 2 + \text{H}]^+$, 700 $[\text{M} + 4 + \text{H}]^+$. **12** had: ^1H NMR, See Table 1; ESI-MS (+) m/z 696 $[\text{M} + \text{H}]^+$, 698 $[\text{M} + 2 + \text{H}]^+$, 700 $[\text{M} + 4 + \text{H}]^+$.

4.5. Biological Assays

4.5.1. Antiviral Assays

Vesicular-stomatitis-virus G protein (VSV-G)-pseudotyped human immunodeficiency virus-1 [63] and replicative dengue virus (obtained from Ralf Bartenschlager) [64] vectors, both expressing the green fluorescent protein (GFP), were used to investigate alkaloids' antiviral properties. The multiplicity of infection (MOI) of HIV-1_{GFP} was assessed by measuring the infectivity of serially diluted vector preparation in Crandell-Rees Feline Kidney (CRFK) cells, while DENV_{GFP} titer was measured by plaque assay in VERO cells.

The monocytic cell line THP-1 derived from an acute monocytic leukemia patient was used in HIV-1_{GFP} infection assays, while the hepatocyte-derived carcinoma cell line Huh7 was used with DENV_{GFP}. Cell viability was evaluated using the Cell-Titer GLO assay kit (Promega, Madison, WI, USA) as previously described [31]. Briefly, 7.5×10^3 Huh7 cells/well or 4×10^4 THP-1 cells/well were seeded in 96-well dark plates and treated with isolated AAs dissolved in methanol at concentrations ranging from 0.05 to 200 μ M for 72 h. Afterwards, Cell-Titer GLO reagent was added in each well of room temperature-equilibrated plates. Luminescence was measured 10 min after shaking the plates for 2 min using a microplate spectrophotometer (Synergy H1, Biotek, Québec, QC, Canada). The percentage of viable cells was calculated at each concentration relatively to cells treated with matched concentrations of MetOH.

To quantify HIV-1_{GFP} and DENV_{GFP} replication inhibition, 4.0×10^4 THP-1 and 7.5×10^3 Huh7 seeded cells per well were treated with indicated concentrations of alkaloids (from 0.05 to 200 μ M) and then infected with HIV_{GFP} at MOI = 0.1 or DENV_{GFP} at MOI = 0.02. After 72 h, the percentage of infected cells was measured using a FC500 MPL cytometer (Beckman Coulter, Inc., Brea, CA, USA) and analyzed with the FlowJo software (BD, FlowJo LLC, Ashland, OR, USA). Matched concentrations of methanol were used as a negative control. Raltegravir was used as a positive control of HIV-1 inhibition, while lycorine was the positive control of DENV inhibition. All experiments were performed three times. CC₅₀ and EC₅₀ values were calculated using QuestGraph IC50 (MLA, Quest Graph™ IC50 Calculator™. AAT Bioquest, Inc., Sunnyvale, CA, USA, <https://www.aatbio.com/tools/ic50-calculator> (accessed on 18 December 2021)).

4.5.2. Cell Culture and Reagents

HaCaT, spontaneously immortalized keratinocytes from adult skin, and AGS gastric adenocarcinoma cells were purchased from Service Cell Line (GmbH, Eppelheim, CLS, Germany). A431 (ATCC-CRL1555) human epidermoid carcinoma cells were from American Type Culture Collection (ATCC, Manassas, VA, USA). All mentioned cell lines were cultured in Dulbecco's Modified Eagle's Medium (DMEM, Sigma Chemical Co., St. Louis, MO, USA) supplemented with 10% fetal bovine serum (FBS, Hyclone Laboratories, Inc. Logan, UT, USA) at 37 °C in a humidified atmosphere of 5% CO₂. Absence of mycoplasma contamination was verified for all cell lines. The purified alkaloids were resuspended in DMSO and added to the cell medium at concentrations varying from 0.5 to 50 μ M as indicated.

4.5.3. MTT Assay

Cell viability was evaluated by measuring the reduction of 3-(4,5-dimethylthiazol-2-yl) 2,5-diphenyltetrazolium bromide (MTT) to formazan by the mitochondrial enzyme succinate dehydrogenase. Briefly, 10×10^3 cells were seeded on 96-well plates and exposed to different concentrations of total extract or metabolites for 48 h. and 72 h. MTT/PBS solution (0.5 mg/mL) was then added to the wells and incubated for 3 h at 37 °C in a humidified atmosphere. The reaction was stopped by removal of the supernatant followed by dissolving the formazan product in acidic isopropanol and the optical density was measured with Synergy H4 microplate reader Gen5 2.07 (ThermoFisher, Waltham, MA, USA) using a 570 nm filter. Under these experimental conditions, no undissolved formazan crystals were observed. Cell viability was assessed by comparing the optical density of the treated samples compared to the controls. Statistical analyses were carried out using the GraphPad Prism version 8.1.2 (<https://www.graphpad.com/scientific-software/prism/> (accessed on 18 December 2021)). Data were represented as the mean standard deviation and analyzed for statistical significance using ordinary one-way analysis of variance (ANOVA) and multiple comparisons. For all tests, $p < 0.05$ was considered to indicate a statistically significant difference.

Author Contributions: Conceptualization, M.M., A.E., I.D.-P. and V.C.; formal analysis, M.M., R.D.L., N.M., M.-P.G., L.B. and I.D.-P.; writing—original draft preparation, M.M., A.E., I.D.-P. and V.C.; writing—review and editing, M.M., N.M., M.-P.G., L.B., I.D.-P., A.E. and V.C. All authors have read and agreed to the published version of the manuscript.

Funding: This work was funded by the Canada Research Chair on plant specialized metabolism Award No 950-232164 to Isabel Desgagne-Penix. Many thanks are extended to the Canadian taxpayers and to the Canadian government for supporting the Canada Research Chairs Program.

Institutional Review Board Statement: Not applicable.

Informed Consent Statement: Not applicable.

Data Availability Statement: Not applicable.

Conflicts of Interest: The authors declare no conflict of interest.

References

1. Nair, J.J.; Bastida, J.; Codina, C.; Viladomat, F.; van Staden, J. Alkaloids of the South African Amaryllidaceae: A review. *Nat. Prod. Commun.* **2013**, *8*, 1335–1350. [[CrossRef](#)] [[PubMed](#)]
2. Christenhusz, M.J.; Byng, J.W. The number of known plants species in the world and its annual increase. *Phytotaxa* **2016**, *26*, 201–217. [[CrossRef](#)]
3. Meerow, A.W.; Snijman, D.A. Amaryllidaceae. In *The Families and Genera of Vascular Plants*; Kubitzki, K., Ed.; Springer: Berlin/Heidelberg, Germany, 1998; Volume 3, pp. 83–110.
4. Evidente, A.; Kornienko, A. Anticancer evaluation of structurally diverse Amaryllidaceae alkaloids and their synthetic derivatives. *Phytochem. Rev.* **2009**, *8*, 449–459. [[CrossRef](#)]
5. Nair, J.J.; van Staden, J. Pharmacological and toxicological insight to the South Africa Amaryllidaceae. *Food. Chem. Toxicol.* **2013**, *62*, 262–275. [[CrossRef](#)] [[PubMed](#)]
6. Jin, Z.; Yao, G. Amaryllidaceae and Scelletium alkaloids. *Nat. Prod. Rep.* **2019**, *36*, 1462–1488. [[CrossRef](#)] [[PubMed](#)]
7. Hartwell, J.L. Plants used against cancer. A survey. *Lloydia* **1967**, *30*, 379–436.
8. Kornienko, A.; Evidente, A. Chemistry, biology, and medicinal potential of narciclasine and its congeners. *Chem. Rev.* **2008**, *108*, 1982–2014. [[CrossRef](#)]
9. Cimmino, A.; Masi, M.; Evidente, M.; Superchi, S.; Evidente, A. Amaryllidaceae alkaloids: Absolute configuration and biological activity. *Chirality* **2017**, *29*, 486–499. [[CrossRef](#)]
10. Bastida, J.; Viladomat, F.; Codina, C. Narcissus alkaloids. In *Studies in Natural Products Chemistry*; Rhahtman, A., Ed.; Elsevier: Amsterdam, The Netherlands, 1998; pp. 323–405.
11. He, M.; Qu, C.; Gao, O.; Hu, X.; Hong, X. Biological and pharmacological activities of Amaryllidaceae alkaloids. *RSC Adv.* **2015**, *5*, 16562–16574. [[CrossRef](#)]
12. Lamoral-Theys, D.; Decaestecker, C.; Mathieu, V.; Dubois, J.; Kornienko, A.; Kiss, R.; Evidente, A.; Pottier, L. Lycorine and its derivatives for anticancer drug design. *Mini-Rev. Med. Chem.* **2010**, *10*, 41–50. [[CrossRef](#)]
13. Lamoral-Theys, D.; Andolfi, A.; Van Goietsenoven, G.; Cimmino, A.; Le Calvé, B.; Wauthoz, N.; Mégalizzi, V.; Gras, T.; Bruyère, C.; Dubois, J.; et al. Lycorine, the main phenanthridine Amaryllidaceae alkaloid, exhibits significant antitumor activity in cancer cells that display resistance to proapoptotic stimuli: An investigation of structure-activity relationship and mechanistic insight. *J. Med. Chem.* **2009**, *52*, 6244–6256. [[CrossRef](#)] [[PubMed](#)]
14. Evdokimov, N.M.; Lamoral-Theys, D.; Mathieu, V.; Andolfi, A.; Frolova, L.V.; Pelly, S.C.; van Otterlo, W.A.; Magedov, I.V.; Kiss, R.; Evidente, A.; et al. In search of a cytostatic agent derived from the alkaloid lycorine: Synthesis and growth inhibitory properties of lycorine derivatives. *Bioorg. Med. Chem.* **2011**, *19*, 7252–7261. [[CrossRef](#)] [[PubMed](#)]
15. Van Goietsenoven, G.; Hutton, J.; Becker, J.P.; Lallemand, B.; Robert, F.; Lefranc, F.; Pirker, C.; Vandebussche, G.; Van Antwerpen, P.; Evidente, A.; et al. Targeting of eEF1A with Amaryllidaceae isocarbostryrils as a strategy to combat melanomas. *FASEB J.* **2010**, *24*, 4575–4584. [[CrossRef](#)] [[PubMed](#)]
16. Van Goietsenoven, G.; Andolfi, A.; Lallemand, B.; Cimmino, A.; Lamoral-Theys, D.; Gras, T.; Abou-Donia, A.; Dubois, J.; Lefranc, F.; Mathieu, V.; et al. Amaryllidaceae alkaloids belonging to different structural subgroups display activity against apoptosis-resistant cancer cells. *J. Nat. Prod.* **2010**, *73*, 1223–1227. [[CrossRef](#)] [[PubMed](#)]
17. Evidente, A.; Kireev, A.S.; Jenkins, A.R.; Romero, A.E.; Steelant, W.F.; Van Slambrouck, S.; Kornienko, A. Biological evaluation of structurally diverse Amaryllidaceae alkaloids and their synthetic derivatives: Discovery of novel leads for anticancer drug design. *Planta Med.* **2009**, *75*, 501–507. [[CrossRef](#)]
18. Van Goietsenoven, G.; Mathieu, V.; Lefranc, F.; Kornienko, A.; Evidente, A.; Kiss, R. Narciclasine as well as other Amaryllidaceae isocarbostryrils are promising GTP-ase targeting agents against brain cancers. *Med. Res. Rev.* **2013**, *33*, 439–455. [[CrossRef](#)]
19. Luchetti, G.; Johnston, R.; Mathieu, V.; Lefranc, F.; Hayden, K.; Andolfi, A.; Lamoral-Theys, D.; Reisenauer, M.R.; Champion, C.; Pelly, S.C.; et al. Bulbispermine: A crinine-type amaryllidaceae alkaloid exhibiting cytostatic activity toward apoptosis-resistant glioma cells. *ChemMedChem* **2012**, *7*, 815–822. [[CrossRef](#)]

20. Govindaraju, K.; Masi, M.; Colin, M.; Mathieu, V.; Evidente, A.; Hudnall, T.; Kornienko, A. Novel topologically complex scaffold derived from alkaloid haemanthamine. *Molecules* **2018**, *23*, 255. [[CrossRef](#)]
21. Pellegrino, S.; Meyer, M.; Zorbas, C.; Bouchta, S.A.; Saraf, K.; Pelly, S.C.; Yusupova, G.; Evidente, A.; Mathieu, V.; Kornienko, A.; et al. The Amaryllidaceae alkaloid haemanthamine binds the eukaryotic ribosome to repress cancer cell growth. *Structure* **2018**, *26*, 416–425. [[CrossRef](#)]
22. Masi, M.; Frolova, L.V.; Yu, X.; Mathieu, V.; Cimmino, A.; De Carvalho, A.; Kiss, R.; Rogelj, S.; Pertsemliadis, A.; Kornienko, A.; et al. Jonquailine, a new pretazettine-type alkaloid isolated from *Narcissus jonquilla* quail, with activity against drug-resistant cancer. *Fitoterapia* **2015**, *102*, 41–48. [[CrossRef](#)]
23. Govindaraju, K.; Ingels, A.; Hasan, M.N.; Sun, D.; Mathieu, V.; Masi, M.; Evidente, A.; Kornienko, A. Synthetic analogues of the montanine-type alkaloids with activity against apoptosis-resistant cancer cells. *Bioorg. Med. Chem. Lett.* **2018**, *28*, 589–593. [[CrossRef](#)] [[PubMed](#)]
24. Ka, S.; Masi, M.; Merindol, N.; Di Lecce, R.; Plourde, M.B.; Seck, M.; Górecki, M.; Pescitelli, G.; Desgagne-Penix, I.; Evidente, A. Gigantelline, gigantellinine and gigancrinine, cherylline and crinine-type alkaloids isolated from *Crinum jagus* with anti-acetylcholinesterase activity. *Phytochemistry* **2020**, *175*, 112390. [[CrossRef](#)] [[PubMed](#)]
25. Houghton, P.J.; Ren, Y.; Howes, M.J. Acetylcholinesterase inhibitors from plants and fungi. *Nat. Prod. Rep.* **2006**, *23*, 181–199. [[CrossRef](#)]
26. Martinez-Peinado, N.; Cortes-Serra, N.; Torras-Claveria, L.; Pinazo, M.-J.; Gascon, J.; Bastida, J.; Alonso-Padilla, J. Amaryllidaceae alkaloids with anti-*Trypanosoma cruzi* activity. *Parasites Vectors* **2020**, *13*, 299. [[CrossRef](#)]
27. Masi, M.; Cala, A.; Tabanca, N.; Cimmino, A.; Green, I.; Bloomquist, J.; van Otterlo, W.; Macias, F.; Evidente, A. Alkaloids with activity against the Zika virus vector *Aedes aegypti* (L.)—crinsarnine and sarniensinol, two new crinine and mesembrine type alkaloids isolated from the south african plant *Nerine sarniensis*. *Molecules* **2016**, *21*, 1432. [[CrossRef](#)] [[PubMed](#)]
28. Masi, M.; van der Westhuyzen, A.E.; Tabanca, N.; Evidente, M.; Cimmino, A.; Green, I.R.; Bernier, U.R.; Becnel, J.J.; Bloomquist, J.R.; van Otterlo, W.A.; et al. Sarniensine, a mesembrine-type alkaloid isolated from *Nerine sarniensis*, an indigenous South African Amaryllidaceae, with larvicidal and adulticidal activities against *Aedes aegypti*. *Fitoterapia* **2017**, *116*, 34–38. [[CrossRef](#)] [[PubMed](#)]
29. He, J.; Qi, W.B.; Wang, L.; Tian, J.; Jiao, P.R.; Liu, G.Q.; Ye, W.C.; Liao, M. Amaryllidaceae alkaloids inhibit nuclear-to-cytoplasmic export of ribonucleoprotein (RNP) complex of highly pathogenic avian influenza virus H5N1. *Influenza Other Respir. Viruses* **2013**, *7*, 922–931. [[CrossRef](#)]
30. Szilávik, L.; Gyuris, A.; Minárovits, J.; Forgo, P.; Molnár, J.; Hohmann, J. Alkaloids from *Leucojum vernalis* and antiretroviral activity of Amaryllidaceae alkaloids. *Planta Med.* **2004**, *70*, 871–873. [[CrossRef](#)]
31. Ka, S.; Merindol, N.; Sow, A.A.; Singh, A.; Landelouci, K.; Plourde, M.B.; Pépin, G.; Masi, M.; Di Lecce, R.; Evidente, A.; et al. Amaryllidaceae alkaloid cherylline inhibits the replication of dengue and Zika viruses. *Antimicrob. Agents Chemother.* **2021**, *65*, e0039821. [[CrossRef](#)]
32. Du Merac, M.L. Systematics and biochemistry of the Amaryllidaceae—Alkaloid content of *Pancratium maritimum*. *Compt. Rend.* **1954**, *239*, 300–302.
33. Cedrón, J.C.; Del Arco-Aguilar, M.; Estévez-Braun, A.; Ravelo, Á.G. Chemistry and Biology of *Pancratium* Alkaloids. In *The Alkaloids: Chemistry and Biology*; Cordell, G.A., Ed.; Elsevier: Amsterdam, The Netherlands, 2010; Volume 68, pp. 1–37.
34. Berkov, S.; Evstatieva, L.; Popov, S. Alkaloids in Bulgarian *Pancratium maritimum* L. *Z. Nat. C* **2004**, *59*, 65–69. [[CrossRef](#)] [[PubMed](#)]
35. Ibrahim, S.R.; Mohamed, G.A.; Shaala, L.A.; Youssef, D.T.; El Sayed, K.A. New alkaloids from *Pancratium maritimum*. *Planta Med.* **2013**, *79*, 1480–1484. [[CrossRef](#)] [[PubMed](#)]
36. Abou-Donia, A.H.; Abib, A.A.; El Din, A.S.; Evidente, A.; Gaber, M.; Scopa, A. Two betaine-type alkaloids from Egyptian *Pancratium maritimum*. *Phytochemistry* **1992**, *31*, 2139–2141. [[CrossRef](#)]
37. Abou-Donia, A.H.; De Giulio, A.; Evidente, A.; Gaber, M.; Habib, A.A.; Lanzetta, R.; El Din, A.A.S. Narciclasine-4-O- β -D-glucopyranoside, a glucosyloxy amidic phenanthridone derivative from *Pancratium maritimum*. *Phytochemistry* **1991**, *30*, 3445–3448. [[CrossRef](#)]
38. Schrader, K.K.; Avolio, F.; Andolfi, A.; Cimmino, A.; Evidente, A. Ungeremine and its hemisynthesized analogues as bactericides against *Flavobacterium columnare*. *J. Agric. Food Chem.* **2013**, *61*, 1179–1183. [[CrossRef](#)]
39. Moeini, A.; Cimmino, A.; Dal Poggetto, G.; Di Biase, M.; Evidente, A.; Masi, M.; Lavermicocca, P.; Valerio, F.; Leone, A.; Malinconico, M. Effect of pH and TPP concentration on chemico-physical properties, release kinetics and antifungal activity of Chitosan-TPP-Ungeremine microbeads. *Carbohydr. Polym.* **2018**, *195*, 631–641. [[CrossRef](#)]
40. Moeini, A.; Mallardo, S.; Cimmino, A.; Dal Poggetto, G.; Masi, M.; Di Biase, M.; van Reenen, A.; Lavermicocca, P.; Valerio, F.; Evidente, A.; et al. Thermoplastic starch and bioactive chitosan sub-microparticle biocomposites: Antifungal and chemico-physical properties of the films. *Carbohydr. Polym.* **2020**, *230*, 115627. [[CrossRef](#)]
41. Antoun, M.D.; Mendoza, N.T.; Ríos, Y.R.; Proctor, G.R.; Wickramaratne, D.M.; Pezzuto, J.M.; Kinghorn, A.D. Cytotoxicity of *Hymenocallis expansa* alkaloids. *J. Nat. Prod.* **1993**, *56*, 1423–1425. [[CrossRef](#)]
42. Boit, H.G.; Döpke, W. Alkaloide aus *Hippeastrum aulicum* var. *robustum*. *Naturwissenschaften* **1960**, *47*, 109.
43. Fales, H.M.; Giuffrida, L.D.; Wildman, W.C. Alkaloids of the Amaryllidaceae. VIII. The Structures of Narcissamine, Pseudolycorine and Methylpseudolycorine. *J. Am. Chem. Soc.* **1956**, *78*, 4145–4150. [[CrossRef](#)]

44. Furusawa, E.; Furusawa, S.; Tani, S.; Irie, H.; Kitamura, K.; Wildman, W.C. Isolation of pretazettine from *Narcissus tazetta* L. *Chem. Pharm. Bull.* **1976**, *24*, 336–338. [[CrossRef](#)]
45. Baxendale, I.R.; Ley, S.V. Synthesis of the alkaloid natural products (+)-plicane and (–)-obliquine, using polymer-supported reagents and scavengers. *Ind. Eng. Chem. Res.* **2005**, *44*, 8588–8592. [[CrossRef](#)]
46. Frahm, A.W.; Ali, A.A.; Ramadan, M.A. ¹³C nuclear magnetic resonance spectra of amaryllidaceae alkaloids. I alkaloids with the crinane skeleton. *Magn. Reson. Chem.* **1985**, *23*, 804–808. [[CrossRef](#)]
47. Bastida, J.; Contreras, J.; Codina, C.; Wright, C.W.; Phillipson, J.D. Alkaloids from *Narcissus cantabricus*. *Phytochemistry* **1995**, *40*, 1549–1551. [[CrossRef](#)]
48. Pabuçcuoglu, V.; Richomme, P.; Gözler, T.; Kivçak, B.; Freyer, A.J.; Shamma, M. Four new crinine-type alkaloids from *Sternbergia* species. *J. Nat. Prod.* **1989**, *52*, 785–791. [[CrossRef](#)]
49. Ghosal, S.; Saini, K.S.; Razdan, S. Crinum alkaloids: Their chemistry and biology. *Phytochemistry* **1985**, *24*, 2141–2156. [[CrossRef](#)]
50. Ma, G.; Li, H.; Lu, C.; Yang, X.; Hong, S. Studies on the alkaloids of Amaryllidaceae. 9. 6-Alpha-Beta-Hydroxy-3-0-Mehylepimaritidine, 2 new alkaloids from *Narcissus tazetta* L. var *chinensis* roem. *Heterocycles* **1986**, *24*, 2089–2092. [[CrossRef](#)]
51. Forgo, P.; Hohmann, J. Leucovernine and Acetylleucovernine, Alkaloids from *Leucojum vernum*. *J. Nat. Prod.* **2005**, *68*, 1588–1591. [[CrossRef](#)]
52. Bastida, J.; Llabrés, J.M.; Viladomat, F.; Codina, C.; Rubiralta, M.; Feliz, M. Narcissus alkaloids, III. 9-O-demethylhomolycorine from *Narcissus confusus*. *J. Nat. Prod.* **1987**, *50*, 199–202. [[CrossRef](#)]
53. Evidente, A.; Lanzetta, R.; Abou-Donia, A.H.; Amer, M.E.; Kassem, F.F. 9-O-Demethylhomolycornine from Egyptian *Narcissus tazetta*. *Archiv. Pharm.* **1994**, *327*, 595–596. [[CrossRef](#)]
54. Evidente, A. Identification of 11-hydroxyvittatine in *Sternbergia lutea*. *J. Nat. Prod.* **1986**, *49*, 168–169. [[CrossRef](#)]
55. Ali, A.A.; Mesbah, M.K.; Frahm, A.W. Phytochemical investigation of *Hippeastrum vittatum*. *Planta Med.* **1984**, *50*, 188–189. [[CrossRef](#)] [[PubMed](#)]
56. Zaragoza-Puchol, D.; Ortiz, J.E.; Orden, A.A.; Sanchez, M.; Palermo, J.; Tapia, A.; Bastida, J.; Feresin, G.E. Alkaloids analysis of *Habranthus cardenasianus* (Amaryllidaceae), anti-cholinesterase activity and biomass production by propagation strategies. *Molecules* **2021**, *26*, 192. [[CrossRef](#)] [[PubMed](#)]
57. King, R.W.; Murphy, C.F.; Wildman, W.C. 6-Hydroxycrinamine and haemanthidine. *J. Am. Chem. Soc.* **1965**, *87*, 4912–4917. [[CrossRef](#)]
58. Wagner, J.; Pham, H.L.; Döpke, W. Alkaloids from *Hippeastrum equestre* Herb.—5. Circular dichroism studies. *Tetrahedron* **1996**, *52*, 6591–6600. [[CrossRef](#)]
59. Bulger, P.; Bagal, S.; Marquez, R. Recent advances in biomimetic natural product synthesis. *Nat. Prod. Rep.* **2008**, *25*, 254–297. [[CrossRef](#)]
60. Habartová, K.; Cahlíková, L.; Rezáčová, M.; Havelek, R. The biological activity of alkaloids from the amaryllidaceae: From cholinesterases inhibition to anticancer activity. *Nat. Prod. Commun.* **2016**, *11*, 1577–1594. [[CrossRef](#)]
61. Berger, S.; Braun, S. *200 and More Basic NMR Experiments: A Practical Course*; Wiley-VCH: Weinheim, Germany, 2004.
62. Pham, L.H.; Döpke, W.; Wagner, J.; Mügge, C. Alkaloids from *Crinum amabile*. *Phytochemistry* **1998**, *48*, 371–376. [[CrossRef](#)]
63. He, J.; Chen, Y.; Farzan, M.; Choe, H.; Ohagen, A.; Gartner, S.; Busciglio, J.; Yang, X.; Hofmann, W.; Newman, W.; et al. CCR3 and CCR5 are co-receptors for HIV-1 infection of microglia. *Nature* **1997**, *385*, 645–649. [[CrossRef](#)]
64. Fischl, W.; Bartenschlager, R. High-throughput Screening Using Dengue Virus Reporter Genomes. In *Antiviral Methods and Protocols*; Gong, E.Y., Ed.; Humana Press: Totowa, NJ, USA, 2013; pp. 205–219.